LEVITATED SUPERCONDUCTING GRAVITY GRADIOMETER FOR PLANETARY MISSIONS. C. E.
Griggs[1], H. J. Paik[1], M. V. Moody[1], S. C. Han[2], D. D. Rowlands[2], F. G. Lemoine[2], P. J. Shirron[3], [1]Department of
Physics, University of Maryland, College Park, MD 20742, [2]Planetary Geodynamics Laboratory, NASA Goddard
Space Flight Center, Greenbelt, MD 20771, [3]Cryogenics and Fluids Branch, NASA Goddard Space Flight Center,
Greenbelt, MD 20771.

Introduction: We are developing a compact tensor
superconducting gravity gradiometer (SGG) for obtain-
ing accurate gravimetric measurements from planetary
orbits. A new and innovative design gives a potential
sensitivity better than 10^{-3} E $Hz^{-1/2}$ (1 E $\equiv 10^{-9}$ s^{-2}) in
the measurement band of 1 mHz to 0.1 Hz for a device
with a baseline just over 10 cm. This is adjustable in
flight down to 10^{-5} E $Hz^{-1/2}$ below 1 mHz, suitable for
detecting time-variable gravity fields on planets.

Significant advances in the technologies needed for
space-based cryogenic instruments have been made in
the last decade. In particular, the use of a cryocooler
will alleviate the previously severe constraint on mis-
sion lifetime imposed by the use of liquid helium, ena-
bling mission durations in the 5-10 year range.

The original SGG, fully developed in the 1990's,
had *mechanically suspended* test masses, which limited
the sensitivity at 1 mHz to ~ 10^{-2} E $Hz^{-1/2}$ with a base-
line nearly 20 cm [1]. *Magnetic levitation* gives a num-
ber of advantages. The resulting magnetic spring is
much more compliant and gives two degrees of free-
dom to each test mass. Hence a tensor gradiometer can
be constructed with only six test masses, and the 10^{-3} E
$Hz^{-1/2}$ sensitivity can be achieved with a device minia-
turized by an order of magnitude in volume and mass.

With 10^{-3} E $Hz^{-1/2}$ sensitivity, the present resolution
of the global gravity field from decades of Doppler
tracking data ($l \sim 110$ for Mars, where l is the maxi-
mum degree of gravity coefficients) could be substan-
tially improved by using SGG data ($l \sim 220$) from a
single spacecraft only within 100 days. It would be
even better than the expected resolution ($l \sim 180$) using
satellite-to-satellite tracking (SST) from two co-
orbiting spacecraft. The more sensitive measurements
from the SGG should also enable mapping the regional
scale of seasonal gravity variations due to mass
transport of CO_2 every month or every season.

The development of a *single-axis* SGG with levitat-
ed test masses started in 2012 with support from
NASA's Earth Science Division. Without provision to
measure linear and angular accelerations in the other
two axes, the common-mode rejection ratio (CMRR) in
this device will be limited to 10^5. Under the present
PICASSO program, we will expand this instrument to
three axes and apply *residual balance* to improve the
CMRR by a factor of 10^3 to 10^8, with a goal to advance
the TRL from 3 to 4.

Principle of Gravity Gradiometry: The second
spatial derivatives of the gravitational potential $\varphi(x_i, t)$
form a gravity gradient tensor Γ_{ij}. Γ_{ij} is symmetric and
its trace is proportional to the local mass density ρ due
to the inverse-square law.

An *in-line*-component gradiometer can be con-
structed by differencing signals between two *linear*
accelerometers whose sensitive axes are aligned along
their line of sight. Likewise, a *cross*-component gradi-
ometer can be constructed by differencing signals be-
tween two concentric *angular* accelerometers whose
moment arms are orthogonal to each other.

In an in-line-component gradiometer, linear and an-
gular accelerations of the platform, a_i and α_i, couple to
the gradiometer through departures from parallelism
and concentricity of the sensitive axes of the accel-
erometers, respectively [2]. There are like error sources
in a cross-component device.

SGG: Both an in-line and a cross-component SGG
have been developed at the University of Maryland
(UM) [1,3].

Basic Accelerometer: Figure 1 shows the principle
of a superconducting accelerometer [4]. The sensing
coil and the SQUID (Superconducting Quantum Inter-
ference Device) input coil are connected to form a su-
perconducting loop. By trapping a large magnetic flux
in the loop, motion of the test mass toward the sensing
coil forces flux out of the sensing coil and into the
SQUID input coil. With a sensing current of 5 A, the
sensitivity to mass motion is ~ 2×10^{-16} m $Hz^{-1/2}$.

In-line-component SGG: Figure 2 is a schematic
circuit diagram for an in-line-component SGG. Two
test masses m_1 and m_2, confined to move along the
baseline (x axis), are connected by a superconducting
circuit. Persistent currents I_1 and I_2 couple the motions
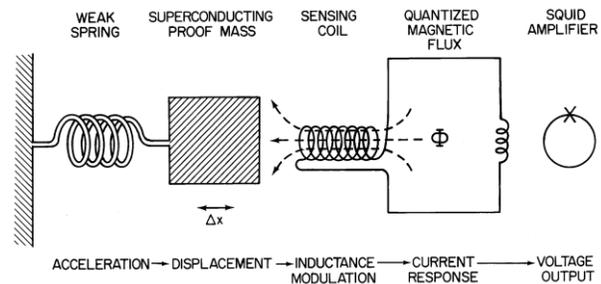of m_1 and m_2, respectively, to the two SQUIDs. The

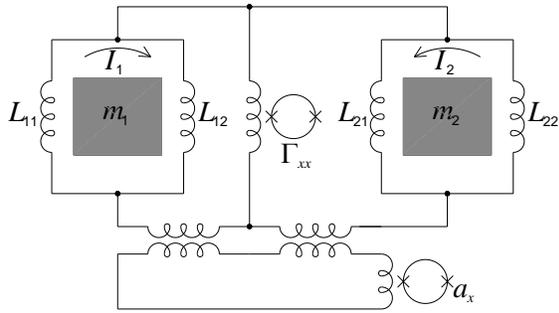**Figure 1. Schematic of a superconducting accelerometer.**

Figure 2. Schematic circuit diagram of in-line-

linear acceleration signals are summed and differenced in the respective SQUIDs to detect a_x and Γ_{xx}, respectively. In an ideal gradiometer with perfectly matched test masses and sensing coils, setting $I_2 = I_1$ would give perfect rejection of the common mode (CM) in the differential-mode (DM) output (Γ_{xx}). In a real device, there are mismatches and I_2/I_1 is adjusted to maximize the CMRR.

Cross-component SGG: Figure 3 shows the configuration of test masses (moment arms) and sensing coils for a cross-component SGG. Two orthogonal arms confined to rotate about a common axis (x) are connected by a superconducting circuit, similar to Fig. 2, to form a gradiometer. As in the in-line-component SGG, I_2/I_1 is adjusted to maximize the CMRR.

Signal differencing by means of stable persistent currents *before* detection is a unique feature of the SGG. **This assures excellent *null stability* of the device, which in turn improves the overall CMRR. The mechanical stability of materials at cryogenic temperatures guarantees that misalignments are also stable.** These error coefficients can therefore be measured once for all during the initial setup, multiplied by the proper acceleration components, and subtracted from the gradiometer output. By applying this 'residual CM balance' [5], the error coefficients have been reduced to $\leq 10^{-7}$ and $\leq 10^{-9}$ for the in-line and cross components, respectively.
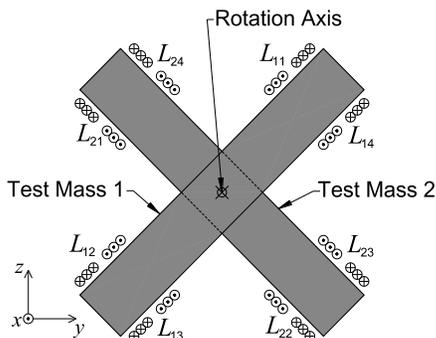
The SGG is a *completely passive* system. There is nothing to control actively, except for the temperature of the device. This greatly simplifies the operation of the SGG.

New Levitation Scheme: A magnetically levitated mass requires five or six degree-of-freedom control, which generally requires levitation coils of elaborate design. A simple levitation scheme, which provides stiff suspension for unwanted degrees of freedom while permitting complete compliance along the sensitive axis, has been devised and demonstrated at UM.

Figure 4 illustrates the principle of levitation by current induced along a superconducting tube. Inside the levitation tube, each of N-turn wires carries current I_L. This induces a screening current on the tube, NI_L, to flow along the inner surface of the tube and return along the outer surface. **The current density on the outer surface is *uniform*, independent of the current distribution inside the tube. This generates a *cylindrically symmetric* magnetic field,** as shown in Fig. 4(a). A tube-shaped superconducting test mass with a bigger diameter surrounds the levitation tube. When the test mass is concentric with the levitation tube, the field is uniform around the levitation tube and does not exert a net force on the test mass. However, if the test mass is displaced radially, as shown in Fig. 4(b), the field becomes stronger at P and weaker at Q, resulting in a radial restoring force.

Tensor SGG: The guiding principle in designing the SGG for laboratory test is the capability to levitate the test masses in 1-g. This led to a test mass design using thin "wings" to produce a light mass ($m = 0.10$ kg). On the ground, a relatively large current (~ 10 A) is required to levitate the test masses against Earth's gravity, and the SGG suffers many g-related errors, such as differential sagging and sensitivity to tilt. **In space, the levitation becomes easier and the g-related errors disappear; thus it should be much easier to reach the intrinsic noise level of the SGG.**

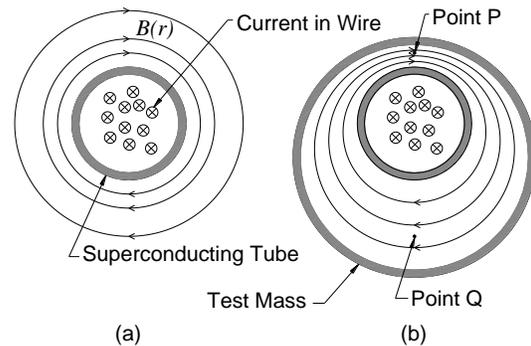Figure 5 is a perspective view of two Nb test masses levitated by a current along a single horizontal Nb

Figure 3. Configuration of the test masses and sensing coils for cross-component SGG.

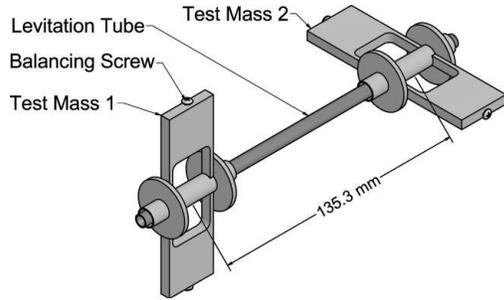**Figure 4. Principle of levitation by current induced on a superconducting tube.**

Figure 5. Two superconducting test masses levitated around a single superconducting tube.

tube. Each test mass has two wings 180º apart, which provide a moment arm about the tube axis (x). A balancing screw is provided at the end of each wing to adjust the center of mass position and bring it to the rotation axis. The current flowing along the tube provides stiff suspension in the radial directions (y and z), but leaves the test masses to move freely along the axis and rotate freely about the same axis. By sensing the differential *linear* and *angular* acceleration of the two masses, one can measure an *in-line* (Γ_{xx}) and a *cross-*component gradient (Γ_{yz}) simultaneously.

Figure 6 is a partially exploded view of the tensor SGG. Six identical accelerometers are mounted on a precision titanium (Ti) mounting cube. The device will measure all six components of the gradient tensor, as well as all six components of the linear and angular accelerations of the platform. The entire SGG assembly weighs 12 kg and fits within a sphere of 20 cm in diameter. Figure 7 is a photograph of the actual Ti mounting cube (10 cm per side) and two Nb accelerometer housings mounted.

All components for a full tensor SGG have been manufactured, including machining Nb test masses and housings. Critical Nb components have been polished
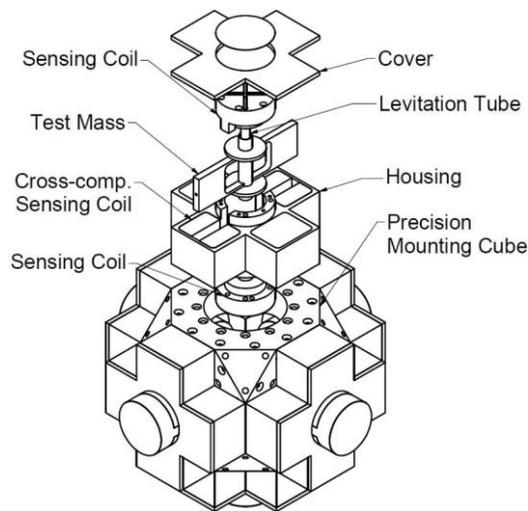

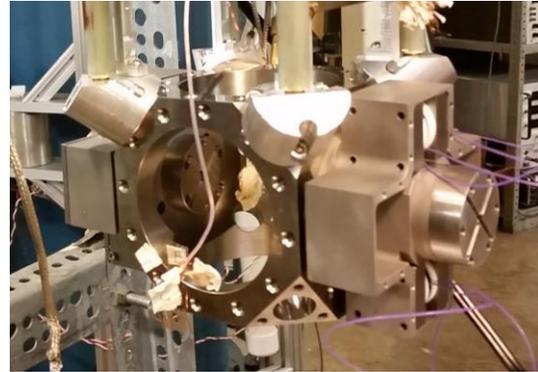**Figure 6. Partially exploded view of the tensor SGG.**

Figure 7. Photograph of the Ti mounting cube (center) and two Nb accelerometer housings.

in order to maximize Q. In addition, sensing coils and heat switches have been constructed. A levitated SGG with a single translation and a single rotation axis is currently being assembled. A cryostat isolation system has been constructed, and means of applying excitations in six degrees of freedom are complete. Figure 8 shows sensing coils used for rotational and translational motion alongside two test masses.

Expected Sensitivities. Figure 9 shows the intrinsic instrument noise spectral density of the *tensor* SGG with the DM resonance frequency f_D tuned to 0.02 Hz. The noise level of the diagonal components is better than 3×10^{-4} E Hz$^{-1/2}$ in the 0.001 to 0.1 Hz frequency band. This represents two orders of magnitude improvement over the performance of the Gravity and Ocean Circulation Experiment (GOCE) gradiometer over a wider bandwidth. The intrinsic noise at $f \leq 1$ mHz can be improved by a factor of 30 by lowering f_D to 0.2 mHz. **An attractive feature of the new SGG is the tunability of f_D in flight by changing persistent currents stored.** f_D can be optimally adjusted for high-resolution static gravity field and for low-resolution time-variable gravity fields, during the mission.
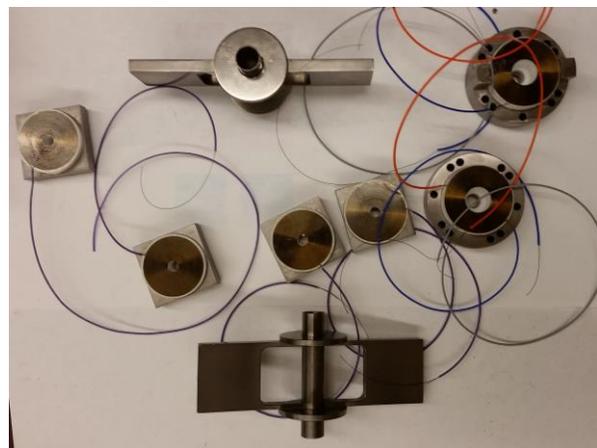

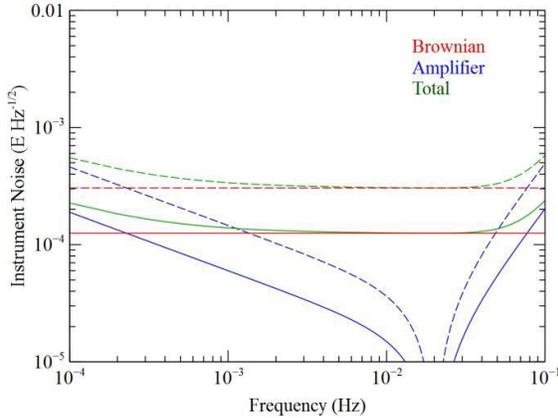**Figure 8. Polished test masses along with sensing coils.**

Figure 9. Intrinsic noise of diagonal (solid lines) and off-diagonal components (dotted lines) of the tensor SGG.

SGG Cryogenic System: The SGG requires stable cooling to ≤ 6 K. For planetary missions, requiring potentially a long cruise phase and extended orbital observations, the cryogenic system will consist of small, highly efficient dewar and a low temperature mechanical cryocooler. The dewar will structurally contain the instrument, using low thermal conductance supports and internal shields to minimize heat leak from the warm spacecraft environment to the cold instrument. The cryocooler will provide direct cooling of the instrument at ≤ 6 K, and the internal shields.

Over the past two decades, development efforts for missions such as Planck and Herschel (ESA), Astro-H (JAXA) and JWST (NASA) have resulted in relatively mature cryocooler technologies that can reach the temperature required for the SGG. For a planetary mission, size and input power are driving considerations, biasing the choice of cryocooler toward those that operate at the highest temperature (within the 6 K limit) and with the highest efficiency. Another critical aspect is the vibration spectrum of the cryocooler, and the potential need for damping structures that isolate the SGG instrument from the exported vibration of the compressors.

Enabled Planetary Science: The global gravity data are indispensable for probing a planet's interior structure from crust to core and its thermal evolution. The planetary gravity data, in conjunction with topography data, are crucial to characterize surface processes such as crater and basin formation, surface and subsurface brecciation, volcanism, tectonics, polar ice, and atmosphere of the planets. Precise mapping of the planet's surface from laser altimetry is impossible without improved knowledge of the orbits that relies almost exclusively on the global gravity information.

At present there is a dearth of detailed geophysical constraints on the nature of the crust and interior of the planets such as Mars and Venus. High-resolution gravity data are crucial to provide our first detailed look at shallow structure, e.g., crustal thickness, layering, mantle structure, as well deeper structure, such as the presence of a lower mantle, and the size and state of the core. Constraining these parameters is essential for understanding the dynamical evolution of the planetary interior, including the thermal state of the lithosphere, past and present transfer of melts to the surface, past magnetic dynamos, and volatile budget of the martian mantle.

The unique high sensitivity of the gravity gradiometer has been demonstrated with the GOCE mission by European Space Agency (ESA) for the Earth [6]. Those measurements were particularly useful to characterize the lithospheric and (steady-state) oceanic processes at an unprecedented spatial resolution, substantially better than the GRACE (Gravity Recovery And Climate Experiment) mission [7] that exploits SST, while the latter has been addressing large-scale time-variability of the global gravity fields that the former is not capable of observing.

The gravity gradiometer technology will bring similar advances to the planet's gravity fields. By virtue of inherent sensitivity to high-frequency gravity signals exceeding the spectrum attainable from Doppler tracking and SST, our gradiometer technology will significantly enhance the resolution of the global gravity field. In addition to the Doppler tracking data, gradiometer measurements will help the trajectory determination of the spacecraft, and thus will improve the quality of surface height measurements from the laser altimeter.

Comparison of SGG, SST, and Doppler Tracking for Planetary Gravity Recovery: The global gravity fields of planetary bodies have been determined on the basis of three different techniques: (1) Doppler tracking of spacecraft from terrestrial tracking stations (typically those of the NASA Deep Space Network), (2) low-low satellite-to-satellite tracking, and (3) gravity gradiometry. All these techniques have been utilized by satellite missions for the Earth and other planets, including, for example, the SST of GRACE and GRAIL (Gravity Recovery And Interior Laboratory) [7,8] and the gravity gradiometry of GOCE [9]. All existing gravity models of the planets except for the Earth and the Moon are presently based upon the Doppler tracking of radio signals between the spacecraft and the ground stations [10].

In order to quantify how much SGG could outperform SST and Doppler tracking, we have conducted global gravity recovery simulation for Mars and Venus in collaboration with R. Pail and R. Rummel, following the semi-analytic approach [11,12]. The noise amplitude spectral density (ASD) from our SGG is described as 1 mE Hz$^{-1/2}$ from 1 mHz to 0.1 Hz and 1/√f noise
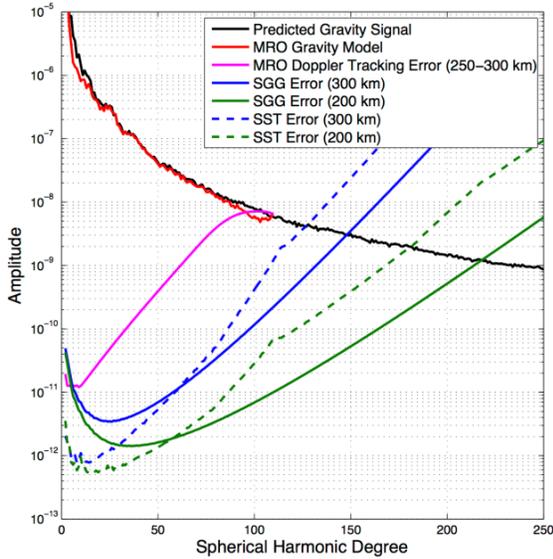
Figure 10. Degree amplitude of the Mars gravity field with the error estimate of the present gravity model for Doppler tracking, SST, and SGG data.

Figure 11. Degreee amplitude of the Venus gravity field with the same error estimates for Doppler tracking, SST, and SGG data as in Fig. 9

below 1 mHz. (We use 3 times worse than our projected sensitivity of 0.3 mE Hz$^{-1/2}$.) For SST, we assumed white range-rate noise of 1 μm s^{-1} Hz$^{-1/2}$ between two satellites separated by ~200 km just like GRACE and GRAIL. Each planet was assumed to be covered globally, which is feasible within less than 100 (Earth) days for Mars and 250 days for Venus. Both 200 and 300 km of altitudes were considered.

Figures 10 and 11 show the current status of Mars and Venus gravity models, respectively, in terms of degree amplitude (equivalent to ASD) from [13,14]. After several decades of nearly continuous tracking of numerous spacecraft, this figure reflects the current state of the art (red and magenta curves for the signal and error estimates, respectively). The signal-to-noise ratio is better than unity globally at harmonic degrees below 95 for Mars and below 75 for Venus. The gravity signal predicted up to very high degrees (depicted as black line) is from the elastic flexure modeling with topography data [15]. The error curves from SST and SGG simulations (blue and green, solid and dashed lines) represent what would be achieved with an independent 100-day data collection episode.

According to Figures 10 and 11, SGG is more sensitive than SST above degree 50, while SST becomes more sensitive below degree 50. However, the low frequency sensitivity of the SGG can be improved by a factor of 30 by tuning f_D down to 0.2 mHz. With such frequency tuning, **SGG outperforms SST at low degrees, where time-varying signals are, as well as at high degrees yielding a superior spatial resolution.**
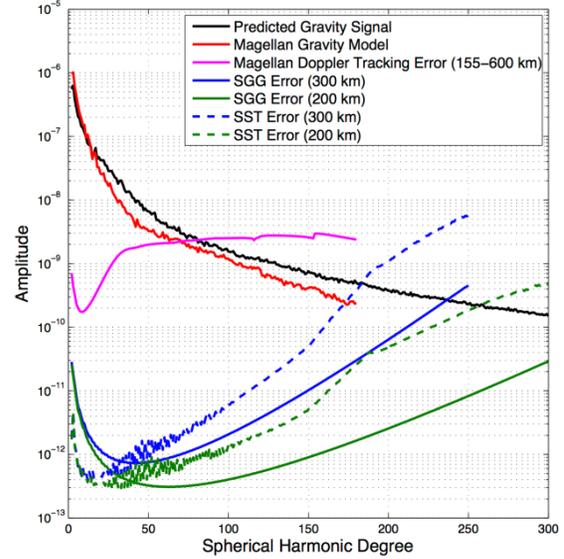
References: [1] Moody, M. V., Paik, H. J. and Canavan, E. R. (2002), *Rev. Sci. Instrum.* **73**, 3957-3974. [2] Chan, H. A. and Paik, H. J. (1987), *Phys. Rev. D* **35**, 3551-3571. [3] Moody, M. V. (2011), *Rev. Sci. Instrum.* **82**, 094501-094513. [4] Paik, H. J. (1976), *J. Appl. Phys.* **47**, 1168-1178. [5] Moody, M. V., Chan, H. A. and Paik, H. J. (1986), *J. Appl. Phys.* **60**, 4308. [6] Drinkwater, M. R. *et al.* (2003), *Earth Gravity Field from Space − from Sensors to Earth Sciences* (Kluwer, Dordrecht, Netherlands), Space Sciences Series of ISSI, Vol. 18, pp. 419-432. [7] Tapley, B.D. *et al.* (2004), *Science* **305**, 503-505. [8] Zuber, M. *et al.* (2012), 43rd Lunar and Planetary Science Conference, abstract #1489. [9] Rummel, R., Yi, W. and Stummer, C. (2011), *J. Geod*, doi: 10.1007/s00190-011-0500-0. [10] Asmar, S. W. *et al.* (2005), *Radio Science* **40**, RS2001. [11] Sneeuw, N. (2000), DG , Reihe C, Dissertationen, Heft Nr. 527, München, ISBN 3769695666. [12] Pail, R. *et al.* (2011), *J. Geod.* doi:10.1007/s100190-011-0467-x. [13] Konopliv, A. S., Banerdt, W. B. and Sjogren, W. L. (1999), *Icarus* **139**, 3-18. [14] Konopliv, A. S. *et al.* (2011), *Icarus* **211**, 401-428. [15] McGovern, P. J. *et al.* (2002), *J. Geophys. Res.,* **107** (E12), 5136, doi:10.1029/2002JE001854.